Diffraction control of subwavelength structured light beams in Kapitza media

Changming Huang,[1,2] Fangwei Ye,[1,2,*] and Xianfeng Chen[1,2]

[1]*Department of Physics and Astronomy, Shanghai Jiao Tong University, Shanghai 200240, China*
[2]*Key Laboratory for Laser Plasma (Ministry of Education), IFSA Collaborative Innovation Center, Shanghai Jiao Tong University, Shanghai 200204, China*
**fangweiye@sjtu.edu.cn*

Abstract: Kapitza tandem structures, consisting of thin alternating layers with opposite signs of the dielectric permittivity, have been recently predicted to afford diffraction arrest of focused microwave radiation [Phys. Rev. Lett. 110, 143901 (2013)]. Here we study the applicability of the Kapitza effect to control the propagation of *structured* subwavelength light beams. We show that a sufficiently deep modulation of the dielectric permittivity allows a nearly complete diffraction cancellation of multiple-peak subwavelength beams, and we study how the degree of diffraction cancellation decreases as the spatial spectrum of the input beam broadens. We also find that subwavelength light beams can be steered by varying the depth of the permittivity modulation. In particular, a sufficiently large permittivity modulation is shown to cause otherwise titled inputs to propagate always along the direction of modulation.

©2015 Optical Society of America

OCIS codes: (050.6624) Subwavelength structures;(260.2710) Inhomogeneous optical media.

References and links

1. H. S. Eisenberg, Y. Silberberg, R. Morandotti, and J. S. Aitchison, "Diffraction management," Phys. Rev. Lett. **85**(9), 1863–1866 (2000).
2. I. L. Garanovich, S. Longhi, A. A. Sukhorukov, and Y. S. Kivshar, "Light propagation and localization in modulated photonic lattices," Phys. Rep. **518**(1-2), 1–79 (2012).
3. W. Cai and V. Shalaev, *Optical Metamaterials: Fundamentals and Applications* (Springer, 2010).
4. N. Engheta, "Circuits with light at nanoscales: optical nanocircuits inspired by metamaterials," Science **317**(5845), 1698–1702 (2007).
5. J. B. Pendry, "Negative refraction makes a perfect lens," Phys. Rev. Lett. **85**(18), 3966–3969 (2000).
6. S. A. Ramakrishna, J. B. Pendry, M. C. K. Wiltshire, and W. J. Stewart, "Imaging the near field," J. Mod. Opt. **50**(9), 1419–1430 (2003).
7. X. Zhang and Z. Liu, "Superlenses to overcome the diffraction limit," Nat. Mater. **7**(6), 435–441 (2008).
8. Y. Xiong, Z. Liu, and X. Zhang, "Projecting deep-subwavelengthpatterns from diffraction-limited masks using metal–dielectricmultilayers," Appl. Phys. Lett. **93**(11), 111116 (2008).
9. G. Ren, C. Wang, G. Yi, X. Tao, and X. Luo, "Subwavelengthdemagnification imaging and lithography using hyperlens witha plasmonic reflector layer," Plasmonics **8**(2), 1065–1072 (2013).
10. P. A. Belov, C. R. Simovski, and P. Ikonen, "Canalization of subwavelength images by electromagnetic crystals," Phys. Rev. B **71**(19), 193105 (2005).
11. X. Li, S. He, and Y. Jin, "Subwavelength focusing with a multiplayered Fabry-Perot structure at optical frequencies," Phys. Rev. B **75**, 045103 (2007).
12. X. Li and F. Zhuang, "Multilayered structures with high subwavelength resolution based on the metal-dielectric composites," J. Opt. Soc. Am. A **26**(12), 2521–2525 (2009).
13. P. Li and T. Taubner, "Multi-wavelength superlensing with layered phonon-resonant dielectrics," Opt. Express **20**(11), 11787–11795 (2012).
14. R. Kotyński, T. Stefaniuk; R. Kotynskiand T. Stefaniuk, "Comparison of imaging with subwavelength resolution in the canalization and resonant tunneling regimes," J. Opt. A, Pure Appl. Opt. **11**(1), 015001 (2009).
15. Z. Jacob, L. V. Alekseyev, and E. Narimanov, "Optical Hyperlens: Far-field imaging beyond the diffraction limit," Opt. Express **14**(18), 8247–8256 (2006).
16. Z. Liu, H. Lee, Y. Xiong, C. Sun, and X. Zhang, "Far-field optical hyperlens magnifying sub-diffraction-limited objects," Science **315**(5819), 1686 (2007).

#233488 - $15.00 USD Received 29 Jan 2015; revised 29 Apr 2015; accepted 29 Apr 2015; published 6 May 2015
© 2015 OSA

17. A. Salandrino and N. Engheta, "Far-filed diffraction optical microscopy using metamaterial crystals: Theory and simulation," Phys. Rev. B **74**(7), 075103 (2006).
18. T. U. Tumkur, L. Gu, J. K. Kitur, E. E. Narimanov, and M. A. Noginov, "Control of absorption with hyperbolic metamaterials," Appl. Phys. Lett. **100**(16), 161103 (2012).
19. I. V. Iorsh, I. S. Mukhin, I. V. Shadrivov, P. A. Belov, and Y. S. Kivshar, "Hyperbolic metamaterials based on multilayer graphene structures," Phys. Rev. B **87**(7), 075416 (2013).
20. A. Poddubny, I. Iorsh, P. Belov, and Y. Kivshar, "Hyperbolic metamaterials," Nat. Photonics **7**(12), 948–957 (2013).
21. L. Sun, J. Gao, and X. Yang, "Giant optical nonlocality near the Dirac point in metal-dielectric multilayer metamaterials," Opt. Express **21**(18), 21542–21555 (2013).
22. D. R. Smith and D. Schurig, "Electromagnetic wave propagation in media with indefinite permittivity and permeability tensors," Phys. Rev. Lett. **90**(7), 077405 (2003).
23. A. Alberucci, L. Marucci, and G. Assanto, "Light confinement via periodic modulation of the refractive index," New J. Phys. **15**(8), 083013 (2013).
24. C. Rizza and A. Ciattoni, "Effective medium theory for Kapitza stratified media: diffractionless propagation," Phys. Rev. Lett. **110**(14), 143901 (2013).
25. C. Rizza and A. Ciattoni, "Kapitza homogenization of deep gratings for designing dielectric metamaterials," Opt. Lett. **38**(18), 3658–3660 (2013).
26. B. Torosov, G. D. Valle, and S. Longhi, "Imaginary Kapitza pendulum," Phys. Rev. A **88**(5), 052106 (2013).
27. C. Huang, F. Ye, Z. Sun, and X. Chen, "Tunable subwavelength photonic lattices and solitons in periodically patterned graphene monolayer," Opt. Express **22**(24), 30108–30117 (2014).
28. E. Forati, G. W. Hanson, A. B. Yakovlev, and A. Alu, "Planar hyperlens based on a modulated grapheme monolayer," Phys. Rev. B **89**, 081410 (R) (2014).
29. COMSOL Multiphysics, *www.comsol.com*.
30. M. Peccianti, A. Dyadyusha, M. Kaczmarek, and G. Assant, "Tunable refraction and reflection of self-confined light beams," Nat. Phys. **2**(11), 737–742 (2006).

1. Introduction

Development of new mechanisms to control diffraction of focused electromagnetic radiation is a central problem in Optics, with implications in a wealth of application areas. Engineered artificial materials with complex refractive index landscapes [1,2] and metamaterials [3] provide wide potential opportunities for diffraction control due to the possibilities afforded by the corresponding spatial dispersion relations that characterize light propagation in the material. Diffraction management is especially interesting at the subwavelength scales, because of its potential applications for signal routing in compact devices [4], subwavelength imaging [5–7], or nanolithography [8,9].

In many schemes involving optical media with a linear response, diffraction management is addressed in structures whose dielectric permittivity varies rapidly along the direction of beam propagation. In some cases, such a rapid permittivity variation allows to use simple effective medium models to describe light propagation, assuming that radiation propagates in an effective homogeneous medium with the averaged dielectric permittivity. Diffractionless propagation of subwavelength beams were reported in inhomogeneous nanostructures designed in such a way, when the spatial dispersion relation yields nearly-flat equal-frequency surfaces for a wide range of spatial frequencies [10–14]. Diffractionless propagation has also been predicted in metal-dielectric stacks with hyperbolic dispersion [15–21], where the effective permittivity can be designed to have opposite signs for different polarizations [22]. However, when the amplitude of modulation of the dielectric permittivity becomes large in comparison with the mean value, a new regime emerges in which the beam evolution is affected not only by the value of the averaged permittivity, but also by additional important contributions arising from the rapidly-varying periodic permittivity oscillations. The appearance and implications of such terms are known as the Kapitza effect, and is a phenomenon that is encountered in several areas of classical and quantum physics. The effect has important implications to light propagation. For example, localized waveguides whose depth is strongly and periodically modulated in the longitudinal direction, have been recently shown to yield light confinement even when the average refractive index contrast vanishes [23]. Importantly, Rizza and Ciattoni predicted earlier in the microwave domain $(\lambda \sim 100\mu\mathrm{m})$ that nearly diffractionless propagation is possible in Kapitza structures, even down to subwavelength scales

#233488 - $15.00 USD Received 29 Jan 2015; revised 29 Apr 2015; accepted 29 Apr 2015; published 6 May 2015
© 2015 OSA

[24]. Diffraction arrest was shown to occur because the rapid, large-amplitude permittivity modulations strongly suppress the longitudinal component of the electric field, thus slowing down diffraction of the transverse magnetic (TM) waves [24–26]. The effect was shown to occur with Gaussian-like beams. However, the ability of the Kapitza effect to suppress diffraction may vary depending on the spatial complexity of the beam, hence on the width of the corresponding spatial spectrum.

2. Model and discussions

In this paper we study the efficiency for diffraction cancellation of the Kapitza effect in the case of *structured* subwavelength light beams featuring closely-packed multiple-peak intensity distributions. Specifically, we study how the diffraction-cancellation efficiency of the Kapitza scheme decreases as the spatial spectral bandwidth of the input subwavelength beams grows. We also study the impact of the Kapitza effect on the propagation angle of titled input beams and its implications for beam steering of subwavelength light.

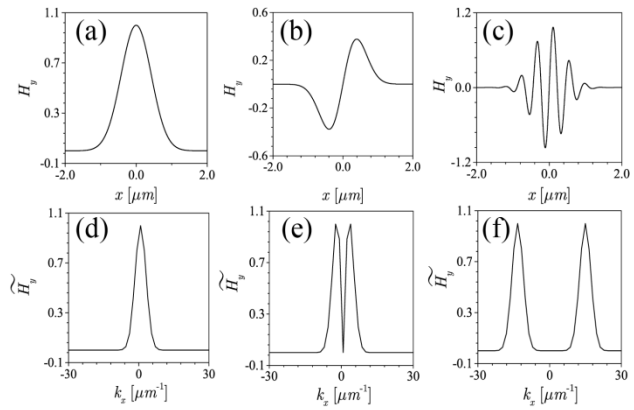

Fig. 1. Magnetic field distributions in the input Gaussian (a) multipole beams with $\Omega = 0.3\pi/w$ (b) and $\Omega = 2.7\pi / w$ (c). The modulus of their spatial spectrums are shown in (d), (e) and (f), respectively. In all cases $w = 600\ \mathrm{nm}$.

Without loss of generality, Kapitza medium here is characterized by smooth periodic variation of the relative dielectric permittivity along the z -axis:

$$\varepsilon(z) = \varepsilon_{\mathrm{bg}} + p\cos(2\pi z/\zeta), \tag{1}$$

where $\varepsilon_{\mathrm{bg}}$ is the relative mean or "background" permittivity; the parameters p and ζ characterize, respectively, the depth and period of the permittivity modulation in the longitudinal z direction. The wavelength of laser radiation $\lambda = 632.8\ \mathrm{nm}$ is chosen from the visible range, while modulation period ζ should be notably smaller than the wavelength λ to guarantee operation in the Kapitza regime [24]. Here we consider the case of $\zeta = 20\mathrm{nm}$ (i.e. $\zeta \sim \lambda/30$), but main results remain qualitatively similar for a broad range of modulation periods as long as the condition $\zeta \ll \lambda$ is satisfied. We also fix mean permittivity value $\varepsilon_{\mathrm{bg}} = 0.1$ that leaves modulation depth p as the only control parameter in Eq. (1). It should be stressed that numerical simulations show that increasing $\varepsilon_{\mathrm{bg}}$ (that can be made comparable with permittivity of some natural materials) requires progressively increasing modulation depths p for the same degree of diffraction suppression for a given light beam. Note that this affords us an additional degree of freedom for the impedance match of the incidence space with that of the Kapitza medium, a condition that has been assumed below. We consider smooth permittivity variations to minimize backward reflections, but the same effect can be observed for step-like $\varepsilon(z)$ profiles, as demonstrated in the final part of the paper. Potentially,

#233488 - $15.00 USD Received 29 Jan 2015; revised 29 Apr 2015; accepted 29 Apr 2015; published 6 May 2015
© 2015 OSA

periodic permittivity landscapes may be fabricated using periodically patterned graphene [27,28], or by stacking metallic and dielectric layers, although in this latter case the scheme will suffer from metallic absorption.

The propagation of the one-dimensional TM-polarized light beams(the only non-vanishing components of the electromagnetic field are E_x, E_z, H_y) in the Kapitza medium is governed by the reduced system of the Maxwell's equations:

$$i\frac{\partial E_x}{\partial z} = -\frac{1}{\varepsilon_0\omega}\frac{\partial}{\partial x}\left(\frac{1}{\varepsilon}\frac{\partial H_y}{\partial x}\right) - \mu_0\omega H_y,$$
$$i\frac{\partial H_y}{\partial z} = -\varepsilon_0\varepsilon\omega E_x, \tag{2}$$

where ε_0 and μ_0 are the vacuum permittivity and permeability, respectively; ω is the frequency of laser radiation, $\varepsilon(z)$ is the relative permittivity of the medium; the field $E_z = (i/\varepsilon_0\varepsilon\omega)\partial H_y/\partial x$ was eliminated from the system (2) for convenience. The beam is allowed to diffract only along the x-axis, while all fields are independent of y. The propagation was modeled using finite element method [29].

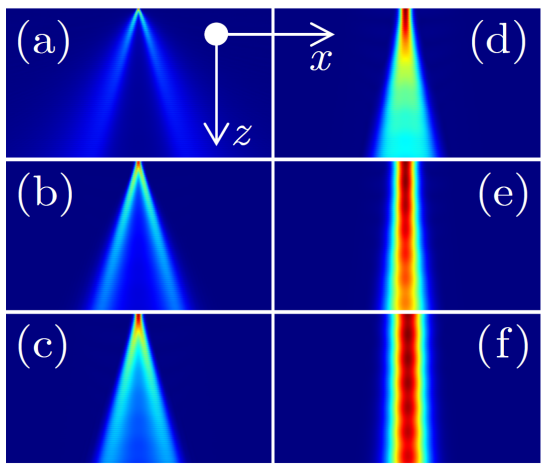

Fig. 2. Evolution dynamics of simple Gaussian beams with width $w = 40\,\mathrm{nm}$ (a), $80\,\mathrm{nm}$ (b), $120\,\mathrm{nm}$ (c), $200\,\mathrm{nm}$ (d), $400\,\mathrm{nm}$ (e), and $600\,\mathrm{nm}$ (f), in the Kapitza medium with modulation depth $p = 1.5$ and modulation period $\zeta = 30\,\mathrm{nm}$. Propagation distance is $10\mu\mathrm{m}$. Note that in Figure 2 and all the other following figures for the propagation simulations, the horizontal and vertical windows are not properly scaled in order to reduce the figure size.

We are primarily interested in the impact of the internal beam structure on the rate of its diffraction broadening in the Kapitza medium. We thus use structured beams with the following initial distributions of the magnetic field:

$$H_y(x)|_{z=0} = \exp(-x^2/w^2)\sin(\Omega x), \tag{3}$$

where w is the width of Gaussian envelope and Ω is the internal modulation frequency. The complexity of the beam shape increases with increase of Ω and decrease of w (see Fig. 1 where profiles of structured beams and their spatial spectrums are compared with that of a simple Gaussian beam). The spatial spectrum becomes wider for larger Ω values. In the case of a uniform medium, this should result in faster diffraction of structured beam, since plane wave components with larger spatial frequencies experience faster dephasing with zero-

#233488 - $15.00 USD Received 29 Jan 2015; revised 29 Apr 2015; accepted 29 Apr 2015; published 6 May 2015
© 2015 OSA

frequency ones. As the width of the envelope w also affects spatial spectrum, it is useful to check first the impact of w on the dynamics of the simplest Gaussian beam.

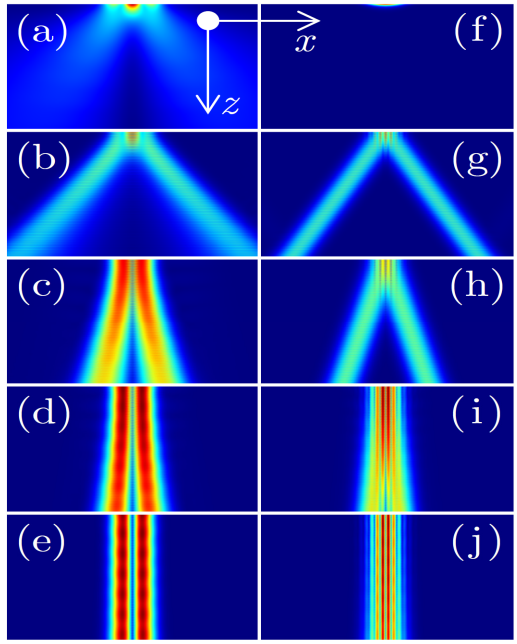

Fig. 3. Evolution dynamics of multipole beams with $w = 600\text{nm}$, $\Omega = 0.3\pi / w$ (a)-(e) and $\Omega = 2.7\pi / w$ (f)-(j) in the Kapitza medium for progressively growing modulation depth of the dielectric permittivity. Panels (a)-(e) correspond to $p = 0, 0.4, 0.6, 0.8$ and 1.5, respectively. Panels (f)-(j) correspond to $p = 0, 0.5, 0.8, 1.7,$ and 3, respectively. Propagation distance is $10\ \mu\text{m}$.

Figure 2 illustrates propagation dynamics of Gaussian beams with widths ranging from $w = 40\,\text{nm}$ (deeply subwavelength regime) to $w = 600\,\text{nm}$ (the borderline regime with $w \approx \lambda$) in the Kapitza medium with a fixed modulation depth $p = 1.5$. Notice that, in all cases the propagation distance of $10\mu\text{m}$ substantially exceeds the Rayleigh length for the beam of width w defined for the effective permittivity $\varepsilon_{\text{eff}} = \varepsilon_{\text{bg}}$ and even for $\varepsilon_{\text{eff}} = \max \varepsilon(z)$. The propagation dynamics is drastically different from the case of a uniform medium. For relatively broad (but still nonparaxial) beams rapid longitudinal modulation of the dielectric permittivity leads to nearly complete diffraction cancellation and conservation of the bell-shaped profiles [Figs. 2(e) and 2(f)]. The regime is exceptionally robust in a sense that even moderate fluctuations in the beam shape and modulation depth do not affect notably the width of the output pattern. At the same time, too narrow beams develop two sidelobes gradually expanding in the course of propagation [Figs. 2(a)-2(c)]. Notice, that rapid and deep oscillations of ε weakly affect local amplitude of the beam, i.e. it evolves on the scale much larger than modulation period ζ. The angle between two sidelobes increases monotonically with decrease of w. Figure 2 shows that the efficiency of diffraction cancellation in the Kapitza medium is determined by the transverse scale of the beam. The impact of w is quantified in Fig. 4(a), where we plot the trapping factor, defined as the ratio $E_{\text{tr}} = U_{\text{out}} / U_{\text{in}}$ of the output at $z = 3\mu\text{m}$ and input $(z = 0\mu\text{m})$ powers $U_{\text{in,out}} = (1/2)\int_{-w/2}^{w/2} E_{\text{x}} H_{\text{y}} dx$ concentrated within the

#233488 - $15.00 USD Received 29 Jan 2015; revised 29 Apr 2015; accepted 29 Apr 2015; published 6 May 2015
© 2015 OSA

transverse window $x \in [-w/2, +w/2]$, as a function of the beam width w. This ratio quickly grows with w and approaches unity already for $w \approx 200\,\mathrm{nm}$.

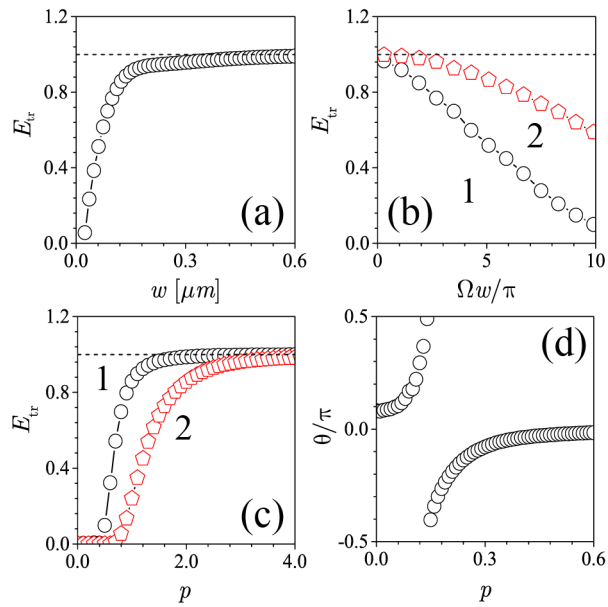

Fig. 4. The ratio of the output and input powers concentrated within $x \in [-w/2, +w/2]$ window (a) versus width of Gaussian beam at $p = 1.5$, (b) versus Ω for complex multipole beam at $p = 1.5$ (curve 1) and $p = 1.5$ (curve 2), (c) versus permittivity modulation depth for complex beams with $\Omega = 0.3\pi / w$ (curve 1) and $\Omega = 2.7\pi / w$ (curve 2). (d) The angle of refraction of tilted Gaussian beam with $\theta_{\mathrm{in}} = 14^\circ$ versus permittivity modulation depth. In panels (b)-(d) the width of the envelope is $w = 600\,\mathrm{nm}$. Horizontal dashed lines in (a)-(c) correspond to $E_{\mathrm{tr}} = 1$ level.

Now we study how efficient the Kapitza medium can arrest the diffraction effects for subwavelength and yet complex structured beams, which is the main goal of the present Letter. The suppression of diffraction for structured dipole and multipole beams upon gradual increase of the permittivity modulation depth p in the Kapitza medium, is illustrated in the left and right columns of Fig. 3, respectively. One can see that irrespectively of the structure of the input beam, rapid diffraction at $p = 0$ [Figs. 3(a) and 3(f)] is replaced by the formation of two sidelobes at moderate p values [Figs. 3(b) and 3(g)], gradual decrease of the angle between sidelobes, and subsequent transition to nearly diffractionless evolution for large modulation depths [Figs. 3(e) and 3(j)]. For a fixed modulation depth p the beam with more complex internal structure (larger internal frequency Ω) always exhibits faster diffraction broadening. This point can be clearly seen by comparing Figs. 3(e) and 3(i): while a modulation depth $p = 1.5$ already well eliminates the diffraction effect for dipole beams, a larger depth $p = 1.7$ is yet insufficient to counteract diffractions for multipole beams. We further quantify the dependence of the trapping factor E_{tr} on the beam complexity Ω in Fig. 4(b). The monotonic decreasing characteristics of the function $E_{\mathrm{tr}}(\Omega)$ clearly reveals that the efficiency of the Kapitza medium in its diffraction cancellations continuously drops if the beam complexity increases. Still, diffractionless propagation can be achieved for arbitrarily complex input patterns, provided that permittivity modulation depth is large enough [Fig. 4(c)]. Saturation of

#233488 - $15.00 USD Received 29 Jan 2015; revised 29 Apr 2015; accepted 29 Apr 2015; published 6 May 2015
© 2015 OSA

E_{tr} at the $E_{\mathrm{tr}} \approx 1$ levels, indicating on the diffraction cancellation, occurs for progressively increasing modulation depths when internal modulation frequency Ω grows.

In all results reported above we assumed that Gaussian or structured beams propagate parallel to the z-axis of the Kapitza medium. Importantly, we found that in the case of tilted inputs the longitudinal permittivity modulation not only suppresses diffraction, but also allows to control the propagation direction inside the periodic medium. In order to illustrate this we consider refraction of the beam impinging on the vacuum-Kapitza medium interface at fixed angle $\theta_{\mathrm{in}} = 14^\circ$ with respect to the z-axis. In this case the angle of refraction strongly depends on the permittivity modulation depth p [Fig. 4(d)]. The angle of refraction θ initially grows with p and reaches large values close to $\pi/2$. Further increase of p is accompanied by an abrupt inversion of sign of the refraction angle and its subsequent gradual reduction. At large permittivity modulations the diffraction is suppressed and the refracted beam always propagates parallel to the z-axis irrespectively of the value of the input angle θ_{in}. Evolution dynamics illustrating various refraction regimes for progressively increasing permittivity modulation depths is shown in Fig. 5. Such giant and controllable beam refraction at the interface of Kapitza medium, far exceeding that available with shallow refractive index modulation [30], may find potential applications for beam steering and routing at the subwavelength scale.

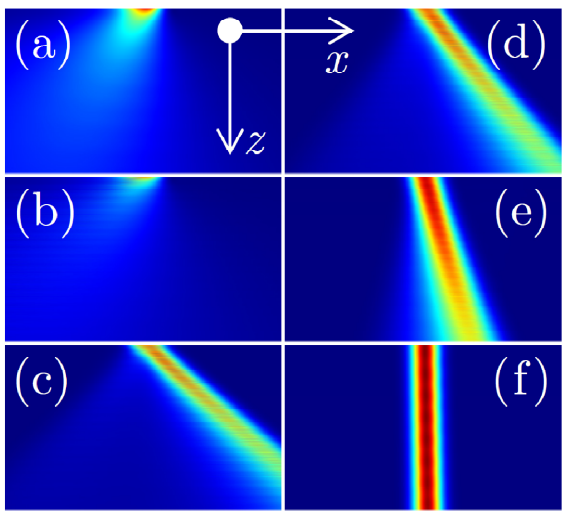

Fig. 5. Propagation dynamics of tilted Gaussian beams with $w = 600\,\mathrm{nm}$, $\theta_{\mathrm{in}} = 14^\circ$ in the Kapitza medium with $p = 0$ (a), 0.06 (b), 0.18 (c), 0.2 (d), 0.3 (e), and 1 (f). Propagation distance is $7.5\mu\mathrm{m}$.

Finally, we note that the Kapitza effects reported above also occur in the layerd metallo-dielectric structures, such as the alternative ultrathin layers of silicon and silvers(Fig. 6(a)) . Figure 6 (d) and 6(e) present a comparative propagation simulation for a dipole and multipole beam input in such a layered Kapitza material; it is evident that the trapping capacity of the Kapitza medium decreases with the increase of the beam complexity (Fig. 6(b)), too. In Fig. 6(c, f, g) we also present the results when silver's losses is taken into account, showing qualitatively similar pictures as in the lossless case. Especialy, we note that the diffractionless propagation in the Kaptiza media is not hamperd by the medium losses.

#233488 - $15.00 USD Received 29 Jan 2015; revised 29 Apr 2015; accepted 29 Apr 2015; published 6 May 2015
© 2015 OSA

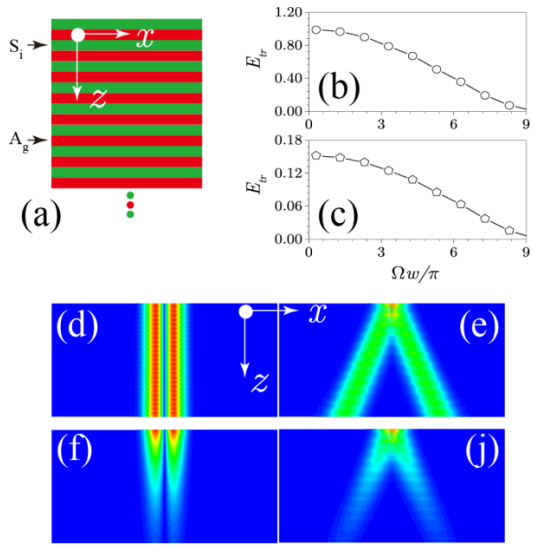

Fig. 6. (a) A schematic of the Kapitza structure composed of alternative layers of silicon and silver, with their thickness $d_{Si} = 17.87$ nm and $d_{Ag} = 10$ nm. Dilectric permittivity of silicon is $\varepsilon_{Si} = 12.25$, while that of silve is $\varepsilon_{\mathrm{Ag}} = -20$ in (b, d, e) and $\varepsilon_{\mathrm{Ag}} = -20 + 0.19i$ in (c, f, j). (b, c) The ratio of the output and input powers. (d, f) $\Omega = 0.3\pi / w$, (e, j) $\Omega = 8.3\pi / w$. Propagation distance in (d-g) is $8.0\ \mu\mathrm{m}$.

3. Conclusion

Summarizing, we showed that, while the rapid large-amplitude modulation of the dielectric permittivity of the material may still suppress diffraction broadening for structured subwavelength beams with arbitrarily complex intensity distributions, the efficiency of the diffraction cancellations lowers down upon the increasing complexity of the beam shape. Small-scale permittivity modulations qualitatively affect refraction at the interface of the Kapitza medium, and sufficiently large modulation redirects all the input beams into the direction of the permittivity of modulations. All these findings were demonstrated in the visible light regime.

Acknowledgments

The work of C. Huang and F. Ye was supported by the National Natural Science Foundation of China (Grant No. 61475101).